Agricultural and Forest Meteorology 372 (2025) 110725

Contents lists available at ScienceDirect

Agricultural and Forest Meteorology

journal homepage: www.elsevier.com/locate/agrformet

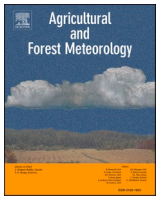

Impact of pollution on the temperature sensitivity of multiple Norway spruce tree-ring parameters in Central Europe

Yumei Jiang [a,b,*], Krešimir Begović [a], Martin Lexa [a], Juliana Nogueira [a], Georg von Arx [c,d], Jan Tumajer [e], Ryszard Kaczka [e], Filip Oulehle [f,g], Nataliya Korolyova [f,h,i], Jesper Björklund [c,d,j], Kristina Seftigen [c,j], Vaclav Treml [e], Rob Wilson [k], Miloš Rydval [a]

[a] Department of Forest Ecology, Faculty of Forestry and Wood Sciences, Czech University of Life Sciences Prague, Kamýcka' 129, 165 00 Prague, Suchdol, Czech Republic
[b] Department of Forest Genetics and Plant Physiology, Umeå Plant Science Centre, Swedish University of Agricultural Sciences, Umeå, Sweden
[c] Swiss Federal Institute for Forest, Snow and Landscape Research WSL, Zuercherstrasse 111, Birmensdorf 8903, Switzerland
[d] Oeschger Centre for Climate Change Research, University of Bern, Bern, Switzerland
[e] Department of Physical Geography and Geoecology, Faculty of Science, Charles University, Prague, Czech Republic
[f] Global Change Research Institute, Czech Academy of Sciences, Brno, Czech Republic
[g] Department of Biogeochemistry, Czech Geological Survey, Prague, Czech Republic
[h] Department of Forest Protection and Entomology, Faculty of Forestry and Wood Sciences, Czech University of Life Sciences Prague, Prague, Czech Republic
[i] The Institute of Forest Ecology of the Slovak Academy of Sciences, Zvolen, Slovakia
[j] Department of Earth Sciences, University of Gothenburg, Gothenburg, Sweden
[k] School of Earth and Environmental Sciences, University of St. Andrews, UK

ARTICLE INFO

Keywords:
Latewood blue intensity
Quantitative wood anatomy
Sulfur/nitrogen deposition
Non-climatic impacts
Climatic signal
Maximum cell wall thickness

ABSTRACT

Central European forests experienced high rates of air pollution in the second half of the 20th century, especially along the borders of Czechia, Germany and Poland. Consequently, tree-growth declines were detected in heavily polluted forests. However, information about how pollution has influenced growth-climate responses beyond tree-ring width (RW) in pollution-affected forests remains sparse. In this study, we investigated the impact of high-level pollution during 1960s-1980s in Central Europe on the climatic signals of various tree-ring parameters of Norway spruce, including RW, latewood Blue Intensity (LWBI), and maximum cell wall thickness (CWT), to understand how tree growth and climatic sensitivity were affected. Tree-ring cores were collected from six temperature-limited high-elevation sites within four pollution-affected regions in Czechia and northern Slovakia. RW and LWBI were measured for all samples and CWT was produced from two sites with contrasting pollution impacts. Distinct pollution-related RW growth suppression was detected in 1970s to 1980s at several sites. LWBI and CWT chronologies were highly correlated (r_{LWBI} = 0.52–0.75; r_{CWT} = 0.63–0.68) with growing season (April-September) temperature and did not exhibit clear signs of distortion by pollution compared to RW (r_{RW} = 0.28–0.58). Pollution stress seemed to reduce tree growth by decreasing cell numbers and made RW less sensitive to climate. This study reveals that impacts of pollution on different tree-ring parameters varied which can further influence their climatic sensitivities. It provides valuable insight in improving the utility of pollution-affected tree-ring chronologies by choosing appropriate parameters, which can ultimately contribute to substantially improving the calibration of climate reconstructions from heavily polluted regions.

1. Introduction

Norway spruce is one of the most dominant and widespread tree species in Central European mountains. However, due to the impact of air pollution and subsequent nutrient soil depletion in the second half of the 20th century, large-scale spruce forest declines have been observed across entire biogeographic regions, especially in the so-called 'Black Triangle' area (Vacek et al., 2020). The Black Triangle spans parts of northern Bohemia (CZ), the southern part of Saxony (DE), and the southwestern part of Lower Silesia (PL) (Abraham et al., 2002). The area

* Corresponding author.
E-mail address: jiang.yumei@slu.se (Y. Jiang).

https://doi.org/10.1016/j.agrformet.2025.110725
Received 16 November 2024; Received in revised form 23 June 2025; Accepted 2 July 2025
Available online 7 July 2025
0168-1923/© 2025 The Authors. Published by Elsevier B.V. This is an open access article under the CC BY license (http://creativecommons.org/licenses/by/4.0/).

has experienced high deposition rates of sulfur and other pollutants leading into the 1990s (above 5 g m^{-2} $year^{-1}$ in 1990; Grubler, 2002). In the Czech Republic, emissions of sulfur dioxide (SO_2) and nitrogen oxides (NO_x) increased sharply from 1950 until the 1980s (Dignon and Hameed, 1989; Smil, 1990; Kopáček and Veselý, 2005). This was followed in the 1990s by a steep reduction in sulfur dioxide pollution due to the desulfurization of lignite-fueled power plants and other industrial facilities (Vacek et al., 2015; Putalová et al., 2019), during which forest recovery was also observed (Kopáček and Veselý, 2005). However, the prolonged effects of pollution on tree growth and forest development remain uncertain.

Atmospheric pollution can impact tree growth both directly and indirectly. Direct impact is related to stomatal uptake of high concentrations of gaseous pollutants, whereas indirect impact can result from the deposition of pollutants due to the chemical reaction between SO_2, NO_X and water, leading to water and soil acidification (Bäck et al., 1995), or light obstruction due to haze (Kirdyanov et al., 2020). These can cause disruption of biogeochemical cycling, which may subsequently lead to nutrient deficiencies and imbalances, ultimately resulting in a decline in tree vitality and growth (Sherman and Fahey 1994). However, the relative importance of direct (pollution in the air) and indirect (deposition, soil acidification and local atmospheric dimming) impacts on tree growth remains a matter of debate (Hruška et al., 2023). In polluted areas, negative growth responses associated with the effects of high pollutant levels complicate the separation of environmental and climatic impacts on growth, potentially distorting growth-climate relationships. Although numerous studies have documented pollution-related growth suppression trends (Kolář et al., 2015; Sidor et al., 2021; Takahashi et al., 2020; Treml et al., 2022; S. Vacek et al., 2015; Z. Vacek et al., 2020), little attention has been given to its effects on climatic sensitivity of tree growth, including potential reversals of the climate signal (Edwards et al., 2022; Ponocná et al., 2018). For optimal climate signal modeling in tree-ring data from historically polluted areas, it is essential to consider environmental pollution as a key non-climatic factor (properly the dominant limiting factor in severe polluted areas) which affects tree growth, especially for the purposes of developing robust dendroclimatic reconstructions.

While annual tree-ring width (RW) has been widely used in dendrochronology, the dendroclimatic utility of this parameter even in climatically sensitive (e.g., temperature-limited) environments can have considerable limitations (Fuentes et al., 2016; Heeter et al., 2019). Thus, a range of alternative techniques has been developed and employed to generate diverse parameters, providing additional datasets that often contain superior climatic information. For example, Blue Intensity (BI) is a technique to generate tree-ring parameters from scanned images of wood samples that represent the reflected light intensity of the wood surface, which is usually closely linked to wood density (Björklund et al., 2024). Among various BI parameters, latewood Blue Intensity (LWBI) has proved to be a more climatically sensitive variable compared to RW, and has also been demonstrated to be largely unaffected by natural disturbance, which represents a common non-climatic growth-influencing factor in many environments (Jiang et al., 2022; Rydval et al., 2018). Quantitative wood anatomy (QWA) is another technique that provides additional sets of tree-ring parameters based on cellular properties derived from high-resolution thin section images, which generally contain stronger and more stable climate signals with fewer biological memory effects compared to most other techniques (Björklund et al., 2023; Seftigen et al., 2022; Lopes-Saez et al., 2023). A comprehensive evaluation of the climate sensitivity and paleoclimatic suitability of BI and QWA in pollution-affected contexts has not yet been conducted. Moreover, diverse wood anatomical parameters derived from QWA technique may also help us to figure out how pollution influences the performance of different tree-ring parameters from the perspective of xylem formation process. Given the greater potential of BI and QWA parameters compared to RW, assessing pollution impacts on these parameters is crucial to identify any pollution-related biases and their effective range. To our knowledge, a comprehensive evaluation of climate sensitivity and paleoclimatic suitability of multiple tree-ring parameters in pollution-affected context has not yet been conducted.

In this study, we aimed to investigate the susceptibility of Norway spruce chronologies developed from various tree-ring parameters (including RW, LWBI and QWA parameters) to pollutants such as sulfur and nitrogen deposition, and its linkages with the xylem formation processes, while also evaluating the suitability of these parameters for dendro-/paleo-climatic applications. To do so, we conducted the study across several representative sites in the Czech Republic and surrounding regions, which experienced varying levels of pollutant deposition during the mid- to late-20th century. By exploring the impacts of pollution on tree-ring chronology trends and climatic signals, we addressed the following key questions: (**I**) How were the chronologies of different tree-ring parameters affected by pollution across space and time, and how did these effects differ among sites with varying pollution timing and intensity? (**II**) Did tree-ring parameters respond differently to pollution, and if so, which parameter was least affected and thus represent the most suitable option for dendroclimatological research in historically polluted areas, and whether such differences were explainable from the perspective of xylem wood formation? (**III**) How has pollution impacted the temperature signal in different tree-ring parameters over time, and can pollution-related biases be removed or minimized?

2. Materials and methods

2.1. Study sites

This research was conducted at six high-elevation Norway spruce sites in the Czech Republic and northern Slovakia, representing four pollution-affected regions (Fig. 1; Table 1). The four regions with the codes of sites representing those regions in brackets include northern Bohemia (NB), the Slovakia-Poland (SP1 and SP2) border, western Bohemia (WB), and south-western Czechia (SWC1 and SWC2), encompassing multiple mountain ranges. The pollution intensity varied somewhat among the six sites, with NB located in northern Bohemia exhibiting the heaviest loading during 1950–2013 (22.4 kg ha^{-1} of sulfur and 18.9 kg ha^{-1} of nitrogen; Table 1). SWC1 and SWC2 in South-western Czechia were exposed to the lowest sulfur deposition intensities in relative terms (8.1 and 7.7 kg ha^{-1} in SWC1 and SWC2, respectively; Table 1). The remaining three sites (SP1, SP2 and WB) were exposed to intermediate levels of pollutant loading compared to the other sites (Fig. 1). Generally, the order of the six sites from most to least polluted was NB > SP1 > SP2 > WB > SWC1 > SWC2 based on the total sulfur deposition data.

These sites occupy environments with a range of climatic conditions. According to the Czech Hydrometeorological Institute (CHMI) meteorological station datasets (Table 1), the annual temperature ranges from −3.81 to 13.5 °C in northern and western Bohemia, and the total annual sum of precipitation ranges from 981 to 1395 mm. Climate conditions in south-western Czechia are colder, with average annual temperature ranging from −4.61 °C to 12.74 °C and the total annual sum of precipitation between 1119 and 1265 mm. The northern Slovakia-Poland border is also relatively colder, and wetter compared to Czech sites according to the Climate Research Unit datasets (CRU TS 4.07; Harris et al., 2020; Table 1). Because the CHMI dataset only covered sites within Czechia, the CRU dataset, which exhibited a high degree of similarity to the CHMI dataset in relative terms, was used for the following analysis.

Historically, atmospheric pollution caused extensive environmental damage in the studied area and surrounding regions, impacting tree growth during most of the second half of the 20th century (Moldan and Schnoor 1992). Large areas (21,000 ha) of high elevation (above 1000 m a.s.l.) spruce forests were damaged (Vacek et al., 2020), particularly during the period of highest acid deposition in the Czech Republic

Table 1
General information about the sampling sites. 'N. tree' represents the number of tree samples which were used to produce RW, LWBI and QWA datasets. 'T_{CRU}' and 'P_{CRU}' are CRU climate dataset with min-max ranges in brackets during the period 1901–2020. 'T_{CHMI}' and 'P_{CHMI}' are spatial interpolated Czech Hydrometeorological Institute (CHMI) meteorological stations dataset with min-max ranges in brackets during the period 1961–2012. 'T' represents the mean annual temperature, 'P' represents the mean value of the summed annual precipitation. 'Sulfur' and 'Nitrogen' are values of the multi-year average deposition for each site during the period 1950–2013. 'Modeled Sulfur' are values of the multi-year average sulfur deposition extracted from the EMEP MSC-W model for the period 1901–2020.

Region	Northern Bohemia	Slovakia-Poland border		Western Bohemia	South-western Czechia	
Site	Jizerské Mts.	Pilsko	Dubrawiska	Klinovec	Šumava-Ostrý	Šumava-Hochficht
Site code	NB	SP1	SP2	WB	SWC1	SWC2
Longitude (°)	15.25	19.32	20.03	13.00	13.56	13.92
Latitude (°)	50.82	49.52	49.24	50.40	48.98	48.74
Elevation (m a.s.l)	930	1384	1650	1050	1210	1320
N. Tree (RW/LWBI)	79	30	12	20	40	20
N. Tree (QWA)	/	/	8	8	/	/
T_{CRU} (°C)	7.70 (5.6–10)	6.86 (4.5–9)		7.31 (5.4–9.5)	6.74 (4.8–8.8)	
P_{CRU} (mm)	663 (489–891)	1067 (809–1467)		667 (457–889)	844 (620–1111)	
T_{CHMI} (°C)	5.15 (−3.81 - 14.23)	/	/	4.53 (−0.60 - 13.50)	3.78 (−4.55 - 12.74)	3.67 (−4.61 - 12.65)
P_{CHMI} (mm)	1395	/	/	981	1265	1119
Sulfur (kg/ha/year)	22.4	15.8	14.5	14.4	8.1	7.7
Nitrogen (kg/ha/year)	18.9	14	12	14.8	13.7	12.8
Modeled Sulfur (kg/ha/year)	27.1	28.1		28.2	20.2	

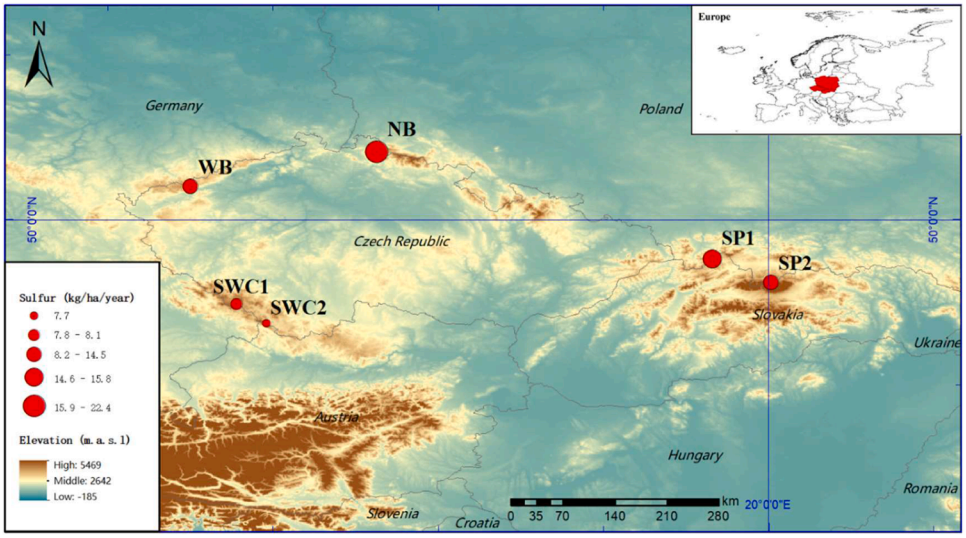

Fig. 1. Map of the sampled tree-ring network in the Czech Republic and the Slovakia-Poland border. The red points represent six sampled sites belonging to four regions, incl. Northern Bohemia (NB), Western Bohemia (WB), South-western Czechia (SWC1, SWC2) and the Slovakia-Poland border (SP1, SP2). Different sizes of the red points represent the multi-year average sulfur deposition for each site during the period 1950–2013.

(Hůnová et al., 2004; Borůvka et al., 2005). Forests in the northern part of the country suffered the most severe growth declines with significant associated mortality events (Rydval and Wilson, 2012; Šrámek et al., 2008). Substantial local damage to spruce stands also occurred in distant areas such as the southwest Czech Republic (Vacek et al., 2019; Krejčí et al., 2013). Moreover, the neighboring area in Poland also faced similar substantial damage to forest stands (Slovik et al., 1995; Modrzyński, 2003).

2.2. Sample collection and tree-ring data measurement

Norway spruce trees that appeared generally healthy (full canopy, no stem damage) were chosen, and single cores were extracted at breast height at each site using a Haglöf increment borer (5 mm diameter). All cores were air-dried, mounted on wooden sample mounts, glued, and sanded. Samples with no apparent discoloration issues were scanned at a resolution of 2400 dpi using an Epson Expression 10,000 XL scanner combined with SilverFast Ai (v.6.6 - Laser Soft Imaging AG, Kiel, Germany) scanning software. Thereafter, both RW and LWBI (Heeter et al., 2022) data were measured from the scanned images using the CooRecorder / CDendro software (Maxwell and Larrson 2021).

2.3. Tree-ring pollution signal detection

The application of a method called Curve Intervention Detection (CID) was explored to help identify the impact of pollution on RW series. CID was used to assess all RW series before detrending to detect the timing and magnitude of potential pollution-related growth anomalies (Druckenbrod et al., 2013; Rydval et al., 2018). A detailed description of the CID method is provided in the supplementary information (Part 1). The CID method is capable of capturing and correcting disturbance-related trends in RW chronologies, potentially reducing their effects on chronology trends (Druckenbrod, 2005; Druckenbrod et al., 2013; Rydval et al., 2015, 2018; Jiang et al., 2022) and improving the climate signal in tree-ring datasets (Rydval et al., 2015, 2018).

While our main analysis focuses on the untreated (non-corrected) RW chronologies, we explored the implementation of this method because pollution-related impacts can result in prolonged growth suppression trends in RW chronologies (Rydval et al., 2012), which can be viewed as a long-term response to a disturbance event. Although severe

pollution typically leads to growth reduction rather than growth release, CID remains applicable as it is capable of capturing these persistent growth suppression patterns.

In addition to the untreated RW chronologies, we also generated two sets of CID-treated RW chronologies to support the detection of pollution effects. The first set used the standard (default) setting (3.29 stdev., cid_def) for disturbance detection, whereas the second set of chronologies employed a more sensitive (2.81 stdev., cid_sen) setting. This more sensitive setting can potentially detect and remove less pronounced disturbance trends that would otherwise remain unidentified with the standard option. However, it is also worth noting that this increased sensitivity may also increase the risk of false positives, which could potentially remove non-disturbance-related (e.g., climatic) signals. Although a third, even more sensitive (2.58 stdev.) setting was also tested, it was not evaluated further since it produced very similar results to the 2.81 stdev. option.

2.4. RW and LWBI detrending

Separate chronologies based on the untreated RW series and two sets of CID-treated RW data (cid_def and cid_sen) were developed following the same standardization approach. RW series were power transformed to stabilize series variance (Cook and Peters, 1997) and detrended by subtraction using the 'spline' method with an 80-year 50 % frequency response in the R package *dplR* (Bunn et al., 2015). To produce RW chronologies, the resulting indices were averaged using Tukey's biweight robust mean.

For the BI datasets, raw blue reflectance measurements were inverted, producing LWBI series that have a positive relationship with wood density and are typically used for direct comparison with climatic variables (Rydval et al., 2014; Björklund et al., 2024). The same 'spline' detrending method and standardization procedure was subsequently also applied to the LWBI series, except for power transformation. All RW and LWBI chronologies were truncated to the period with a minimal replication 10 series to ensure chronology robustness for analysis. We also calculated the expressed population signal (EPS) for RW and LWBI data to evaluate the strength of the common signal (Table S1). We also examined relationships between first-differenced RW and LWBI chronologies and instrumental temperatures to assess interannual signal changes.

2.5. QWA data generation and processing

Considering that QWA parameter production is more time-consuming, a subset of 16 samples, 8 from each of two sites (WB and SP2), were selected for QWA sample preparation and wood anatomical parameter analysis. These sites represent two geographically distinct areas at the western and eastern extremes of the study network, both of which were exposed to high pollution levels in the late 20th century. WB is situated within the Black Triangle area, and SP2 locates in Tatra National Park (Fig. 1). While both sites experienced seemingly similar pollution histories (Fig. 1; Table 1), they exhibited contrasting growth (RW) responses during the period of peak emissions (Fig. S2). The selected cores were first cut into small pieces (length ~ 2 cm) and then refluxed with ethanol (99.5 %; Campbell et al., 2011) using a Soxhlet apparatus for 12 h to remove extractives (resins). Then, samples were individually processed using a mix of alcohol and xylol, followed by paraffin embedding in cassettes, and then cut into thin sections of 12 μm thickness using a rotary microtome with Feather N35 histological blades (Gärtner et al., 2015; von Arx et al., 2016). Sections were then stained with a mixture of safranin and astra blue to increase contrast, and permanently fixed on glass slides with Canada balsam (Björklund et al., 2020; von Arx et al., 2016). Permanent slides were dried in an oven at 60 °C for 12 h and then digitized using a slide scanner (ZEISS Axio Scan.Z1) with associated image processing software (ZEISS ZEN 3.4, blue edition). The program ROXAS v3.0 (von Arx and Carrer, 2014) was used to detect and measure anatomical structures of tracheid cells and annual ring borders semi-automatically. The cell detection algorithms of a deep-learning model that will be part of ROXAS AI (Katzenmaier et al., 2023) have also been used to feed back to the data generation pipeline of the traditional ROXAS version to obtain higher-quality data.

While a broad range of anatomical parameter datasets (e.g., cell wall area, cell wall thickness, lumen area, etc.) were generated, the subsequent analysis primarily focused on the parameters most relevant for dendroclimatological research, following an initial screening of various QWA parameters (Fig. S3) and additional examination (Fig. S4). 'Maximum average (mean of tangential and radial) cell wall thickness' (hereafter CWT) was identified as the most temperature-sensitive parameter, and subsequent analyses concentrated predominantly on this feature. The temperature sensitivity of the CWT chronologies was evaluated based on two aggregation approaches (median and 75th percentile) and a range of bandwidth settings (from 10 to 120 μm; Fig. S5). The version with the strongest correlation to temperature (75th percentile and 10 μm) was selected as the most climatically sensitive, and the temporal stability of this temperature signal was then assessed. In accordance with RW and LWBI, the 80-year spline detrending method (without power transformation) was applied to the QWA parameter chronologies, and the temperature sensitivity of the CWT chronologies was examined across different pollution impact periods. The same detrending approach was used for all tree-ring parameters to minimize methodological differences, ensuring consistent treatment and comparability among the datasets. We additionally explored the changing patterns of some relevant QWA parameters under pollution stress and try to find out the growth reactions to pollution regarding xylem wood formation, including earlywood (EWW) and latewood (LWW) width calculated from the QWA dataset, cell count and density, median of total cell area (TCA) for the earlywood (EW_TCA) and latewood (LW_TCA), and ratios of median lumen area to total cell area for the earlywood and latewood.

2.6. Exploration of pollution impacts on tree-ring chronology temperature signals

To assess the potential impact of pollution on climatic signals in different tree-ring parameters, responses of RW, LWBI and CWT chronologies to climate variables were assessed using the Pearson correlation coefficient (r) with the package *treeclim* in R (Zang and Biondi, 2015). The growth-climate response was assessed for the common "Full period" (1930–2008), and three distinct periods representing varying exposure to pollution, defined as "Pre-pollution" (1930–1959), "Peak pollution" (1960–1989), and "Post-pollution" (1990–2008), approximately corresponding to the periods before, during and after the temporal span associated with high rates of pollutant deposition based on the sulfur / nitrogen deposition history (Fig. 2c, d; Fig. S1a) and literature records (Dignon and Hameed, 1989; Smil, 1990; Kopáček and Veselý, 2005). To assess possible changes in the climatic signal in more detail, its temporal stability was quantified using a 31-yr running correlation between the tree-ring chronologies and optimal seasonal temperature variables which were identified based on monthly / seasonal growth-climate response analyses. Climatic time series were extracted from the CRU TS 4.07 (0.5°) gridded monthly dataset (Harris et al., 2020) covering the period 1901–2020. To ensure consistency and enable a direct comparison of tree-ring and temperature data over the same timescales, the same 80-year spline method used to standardize the tree-ring datasets was also applied to detrend the temperature series before the growth-climate response analysis (Fig. S1). This removed longer trends in the temperature data that were not retained in the tree-ring chronologies due to detrending (Ols et al., 2023). The climatic response of CID-treated RW chronologies (RW_cid_def / RW_cid_sen) was also assessed over the "Full period".

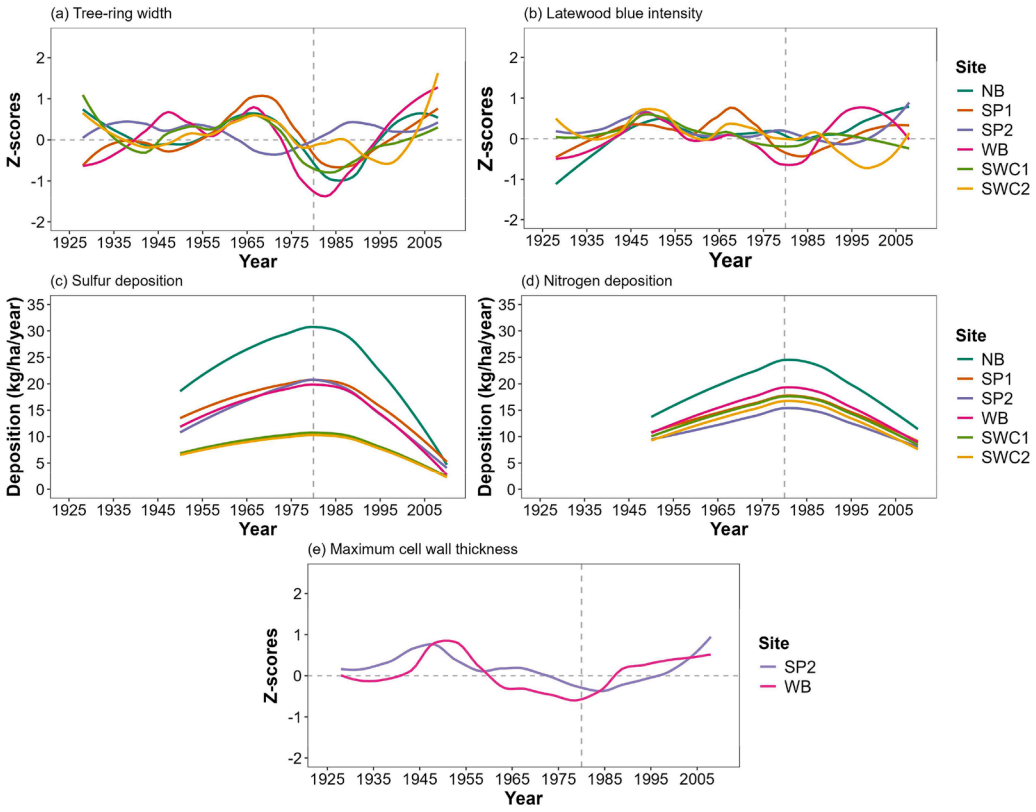

Fig. 2. Long term growth trends of trees represented by different tree-ring parameters and pollution history of all studied sites, with (a) and (b) displaying the tree-ring width (RW) and latewood Blue Intensity (LWBI) chronologies, respectively, (c) and (d) illustrate the sulfur and nitrogen deposition for the period 1950 to 2013, (e) shows chronologies of the maximum cell wall thickness (CWT) of the two sites WB and SP2. All chronologies were z-scored within the common period (1928–2008) where replication equals or exceeds 10 series (except for CWT with replication of 8) (Table S1). The curves represent smoothed values using the 'loess' method (with parameters set to $n = 80$, span = 0.4) in the R package 'ggplot2'. Purely z-scored chronologies after 1900 without trend removal can be found in the Supplementary materials (Fig. S2). Vertical dashed lines mark the year 1980 when average sulfur and nitrogen deposition values (c and d) reach the highest levels.

2.7. Pollution intensity and tree growth relationships

To assess pollution loading over space and time among sites, we used two types of pollution datasets for these comparisons. The first dataset represents the annual sulfur deposition which was extracted from the EMEP MSC-W model for the 1901–2020 period for the four regions (Table 1; Fig. S1a; Engardt et al., 2017), covering all study sites. The second dataset contained both sulfur and nitrogen deposition records for the period 1950–2013 and was estimated using the method introduced in Oulehle et al. (2016). Both pollution datasets indicate that our study sites were heavily exposed to sulfur and nitrogen deposition during the 1960–1990s period, with the peak centered around the year 1980, and a gradual decline thereafter (Fig. 2c, d; Fig. S1a; Fig. S2c, d). Tree-ring chronologies were compared with pollution loading to assess potential links between pollution levels and various tree-ring parameters (Kolář et al., 2015). A simple linear regression model (Bangdiwala, 2018) was applied to test the overall relationship between the chronologies and pollutant loadings.

3. Results

3.1. Tree growth trends of different tree-ring parameters

RW chronologies of most sites revealed growth declines around the 1980s to varying extent, particularly for sites NB, and WB (Fig. 2a; Fig. S2a), coinciding with the period of peak pollutant deposition (Fig. 2c, d). Compared to RW, the LWBI chronologies exhibited less temporal variability, with most sites (i.e., NB, SP2, SWC1, SWC2) showing near-average index values throughout the Peak pollution period of the 1980s (Fig. 2b; Fig. S2b). Exceptions were SP1 and WB, which experienced declines in the late 1970s. The most prominent and prolonged LWBI chronology decline was observed for SWC2 around the late 1990s. Similar to LWBI, the two CWT chronologies (WB and SP2) showed relatively stable trends over time, although both sites did contain low index value trends around the 1970s and 1980s (Fig. 2e; Fig. S2e, f).

3.2. Detected and corrected tree-ring pollution signals

The effectiveness of applying the CID method for pollution signal detection and correction to RW chronologies varied among sites and detection sensitivity settings, with the most prominent suppression trends being corrected in NB and WB during the 1970s to 1980s, especially by the more sensitive CID setting (cid_sen; Fig. 3a, d). In contrast, only marginal differences in chronology structure were observed for the two sites at the Slovakia-Poland border (SP1 and SP2) when comparing the growth trends before and after CID processing. Additionally, another apparent suppression trend was detected in SWC2 (Fig. 3f), although it occurred in a different period (around the mid-1990s).

3.3. Temperature sensitivity of tree-ring metrics in different pollution intensity periods

Growth-climate responses varied considerably among sites and tree-ring parameters. Temporal variations in temperature signals were particularly evident in RW chronologies (Fig. 4). Over the Full period, RW correlated most strongly ($r = 0.43$–0.58; $p \leq 0.01$) with June-July temperature at sites SP1, SP2, and SWC2, whereas April-August

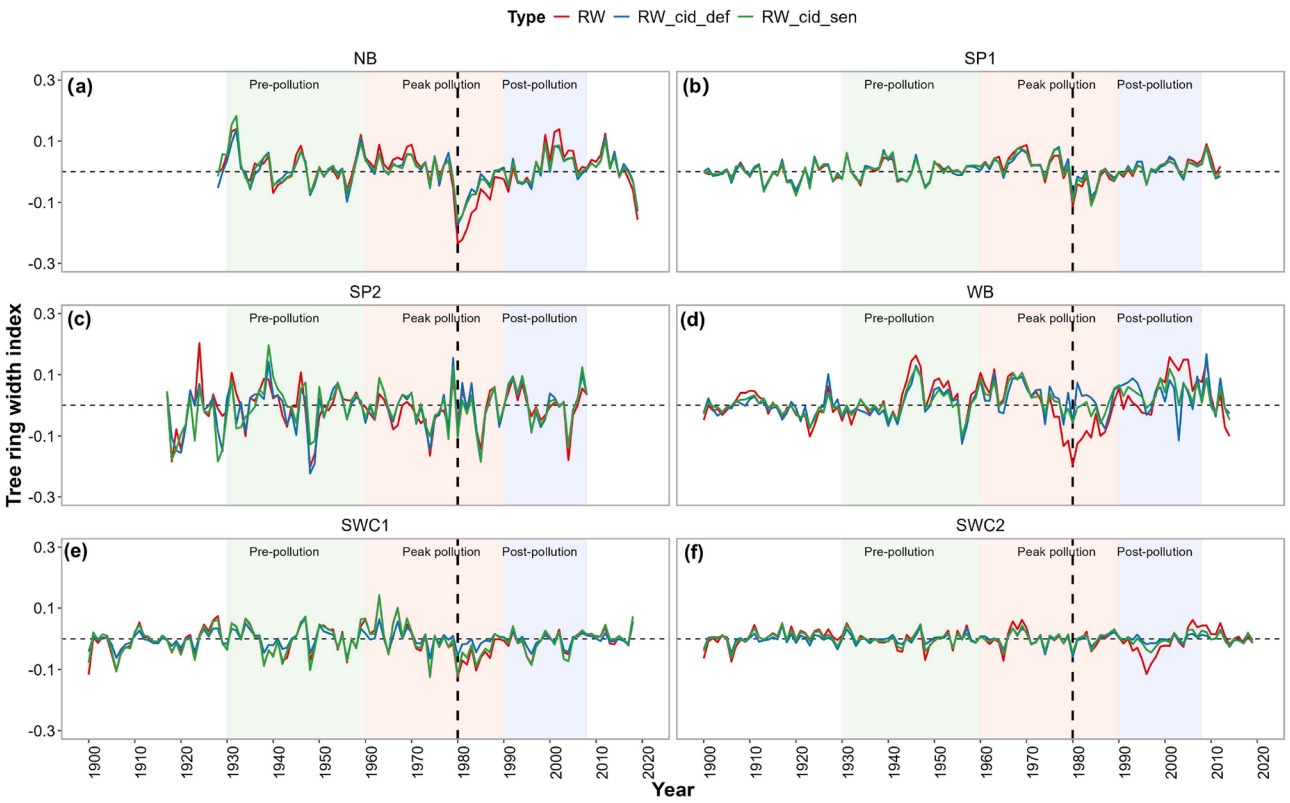

Fig. 3. Tree-ring width (RW) chronologies before and after applying the curve intervention detection (CID) method with both default (cid_def) and sensitive (cid_sen) detection thresholds. Vertical dashed lines mark the year 1980, which corresponds to peak pollutant deposition and the year in which most sites exhibit the lowest RW chronology index value. Chronology replication for all sites reaches or exceeds 10 series throughout the presented period. Different color shaded areas represent different pollution periods, they are Pre-pollution (1930–1959), Peak pollution (1960–1989) and Post-pollution (1990–2008) from left to right.

temperature was most strongly correlated ($r = 0.28$–0.45; $p \leq 0.01$) with the NB and WB chronologies. In contrast, temperature signals in LWBI chronologies were considerably stronger and more representative of the entire spring-summer growing season. April-September temperature correlated most strongly ($r = 0.52$–0.75; $p \leq$ l0.01) with LWBI for all sites (Fig. 4b). For RW, the average strength of the temperature signal was significantly positively related to site elevation, whereas no such relationship was observed for LWBI chronologies (Fig. S6).

Considering the three evaluated periods, RW temperature signals at the Czech sites (NB, WB, SWC1, SWC2) generally weakened during the Peak- and Post-pollution periods, whereas no such weakening occurred at the Slovakia-Poland (SP1, SP2) sites during Peak pollution, and only SP1 showed a weaker relationship in the Post-pollution period (Fig. 4a). Running 31-yr correlations between the RW chronologies and instrumental temperature over the Full period also showed considerable spatial and temporal variability in RW temperature signals. The most prominent signal decline from the Pre- to Post-pollution period occurred with sites NB and WB, while other sites showed more stable relationships over time (Fig. 5a, d – light grey bars and red curves). High-frequency (interannual) relationships were generally stronger but also closely mirrored those of the 80-year spline chronologies. Notably, however, NB and WB retained stronger temperature signals around the 1980s followed by a more pronounced weakening in the Post-pollution period (Fig. S7a, d). While modest, CID correction produced some minor improvements in temperature signal strength in both the default (RW_cid_def) and sensitive (RW_cid_sen) RW chronology versions for sites NB, WB, SP2, and SWC2 in the Peak pollution period (Fig. S8, S9).

In contrast to RW, the LWBI temperature signals were considerably more stable across all pollution intensity periods for most sites. The seasonally broader (April-September) LWBI signals generally remained consistently strong throughout the last century, with little to no weakening even during the heavy pollution period (1960–1989; $p< = 0.01$; dark grey bar in Fig. 5). The only exceptions were NB in the Pre-pollution period and SWC1 and SWC2 in the Post-pollution period, where correlations were non-significant.

Similarly to LWBI, the CWT chronologies contained a generally strong and broad (April-September) growing season temperature signal ($r = 0.63$ - 0.68; $p< = 0.01$ over the Full period). Both WB and SP2 chronologies remained largely stable over time, apart from a weaker signal in WB during the Post-pollution period (Fig. 4c). The temporal patterns of the CWT temperature signals behaved similarly to LWBI, maintaining strong and stable relationships (Fig. 5c, d - black bars and green curves).

3.4. Agreement between tree-ring chronologies and temperature trends

When comparing the trends of tree-ring chronologies with instrumental temperature series, a clear divergence of RW chronologies for NB and WB from the temperature series is evident around the 1980s (Fig. 6a). Furthermore, RW trends at WB (and, to a lesser extent, NB) were consistently higher compared to their respective temperature series before ~1970 and after ~2000, making these trend departures even more pronounced. However, these patterns were not observed in LWBI chronologies, which maintained strong agreement with their respective temperature series, closely tracking instrumental temperatures at nearly all sites and time periods (Fig. 6b). Notably, the lower LWBI index values in the late 1970s coincided with a period of lower temperatures. The only exception was SWC2, which showed a distinct negative deviation from temperature in the 1990s that was also apparent, though less pronounced, in its RW chronology. Maximum CWT chronologies showed a similar high degree of agreement with instrumental temperatures, including at WB where its RW counterpart showed an anomalous

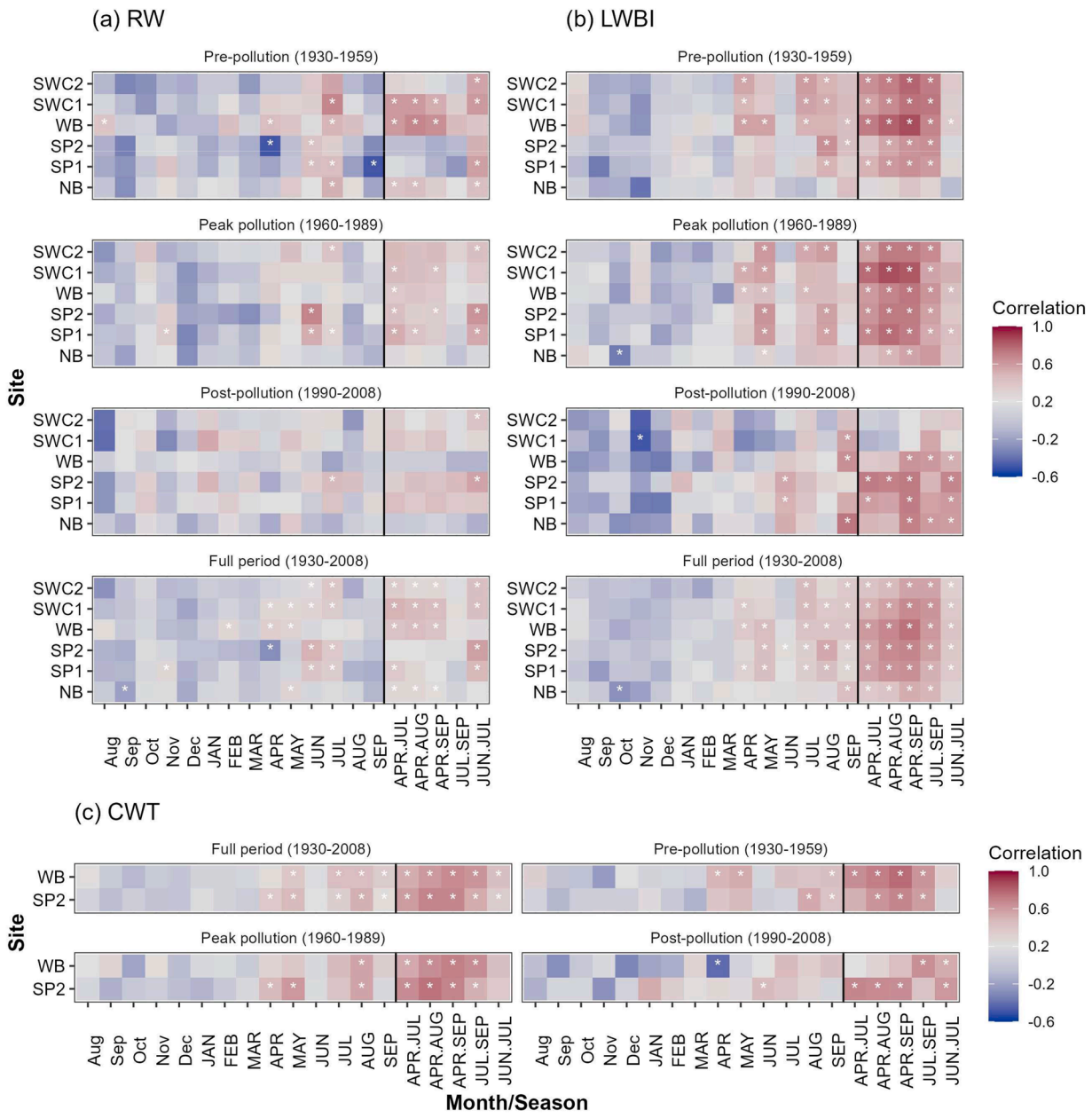

Fig. 4. Growth-climate correlations between (a) tree-ring width (RW), (b) latewood Blue Intensity (LWBI), (c) maximum cell wall thickness (CWT), and CRU monthly / seasonal temperature for different temporal periods. The sites are ordered by increased total sulfur deposition between 1950–2013 from top to bottom (Table 1). X-axis names with only the first letter capitalized indicate months of the previous year relative to the growth year. Correlations to the right of the solid vertical black lines represent seasonal ranges, with the first and last months of each range indicated. The asterisks (*) indicate correlations that are statistically significant at the 0.01 significance level.

deviation from temperature trends (Fig. 6c).

3.5. Variations in wood anatomical parameters under pollution stress

A detailed examination of various QWA parameter chronologies from the WB and SP2 sites revealed both similarities and differences in their wood anatomical properties over time (Fig. 7). Raw ring width properties, including full RW, earlywood width (EWW) and latewood width (LWW), showed contrasting patterns between the two sites. SP2 approximately followed a characteristic negative exponential pattern, whereas WB displayed considerably larger absolute ring sizes and higher temporal variability (median full RW range: WB = ~400–2300 mm, SP2 = ~200–900 mm). At WB, all ring width metrics were large during the Pre-pollution period, reduced sharply during the latter part of the Peak pollution period (particularly around the 1970s and 1980s), and increased again in the Post-pollution period (Fig. 7a). In contrast, SP2 exhibited a gradual RW decrease from the Pre-pollution to Peak pollution period, followed by a stable and slightly increasing trend in the Post-pollution period (Fig. 7e). Cell counts at both sites mirrored these ring-size patterns, while cell density remained generally stable over time. However, modestly higher cell density was observed at both sites in the 1980s, with SP2 also displaying higher values in the early 1900s; Fig. 7b, f).

At WB, earlywood total cell area (EW TCA) showed below-average values in the 1980s (EW $TCA_{1980–1989}$ = 1041) and 1990s, though similar low values were also observed in the early 20th century (Fig. 7c). This was followed by an increase in the 2000s (EW $TCA_{2000–2008}$ = 1236), exceeding the long-term average (EW $TCA_{1900–2008}$ = 1113).

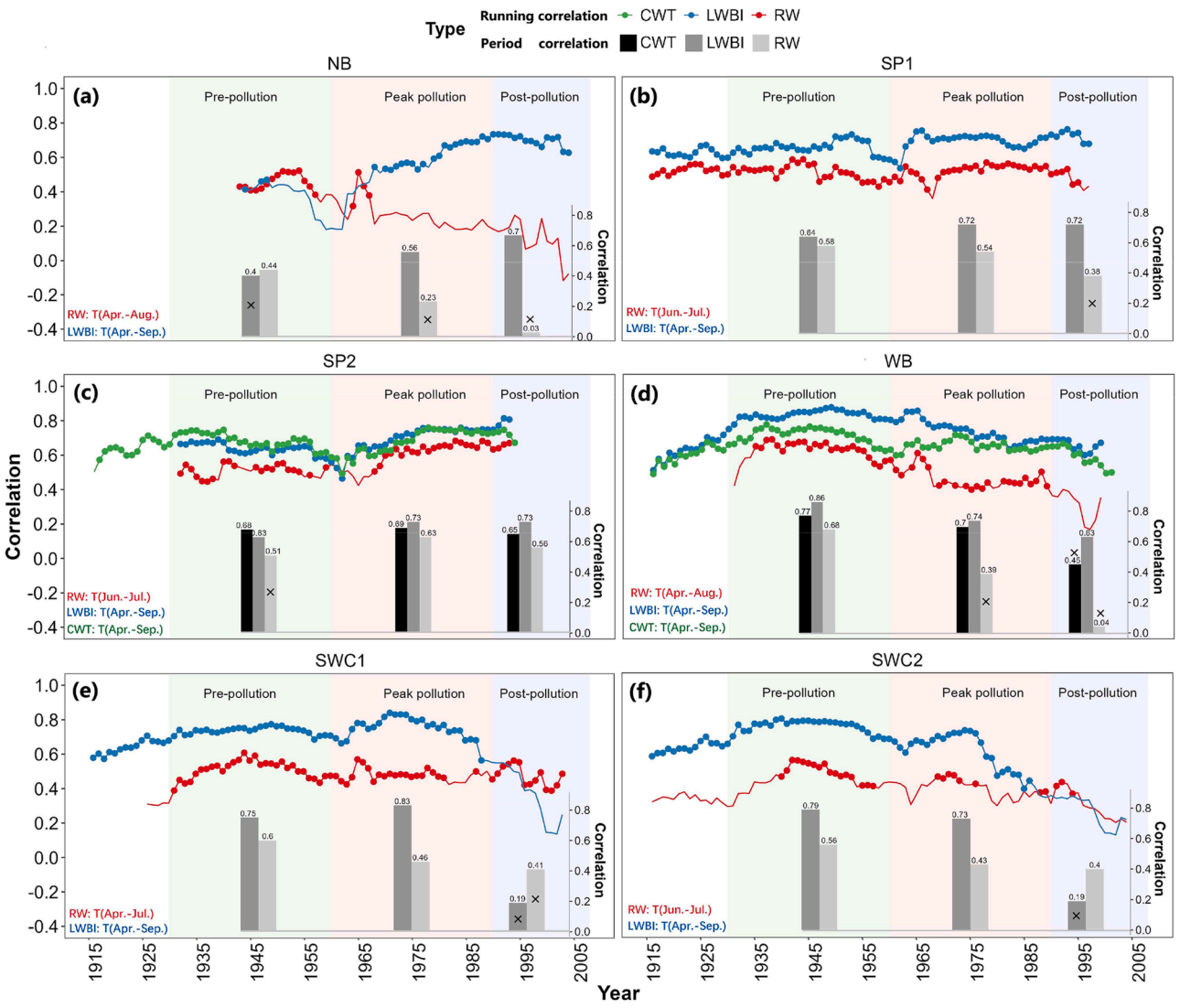

Fig. 5. Running correlations with a 31-year window between chronologies of tree-ring width (RW), latewood Blue Intensity (LWBI), maximum cell wall thickness (CWT) and optimal seasonal temperatures for each site and parameter identified in Fig. 4, with 'T' and the abbreviated month name mean temperature and the months of the year, e.g., T(Apr.-Aug.) corresponds to April-August mean temperature. The dots on the line plots indicate significant correlations with a significance level of 0.01. Correlations values represent the middle year of the 31-year running correlation periods along the x-axis. Chronology replication for all sites reaches or exceeds 10 series throughout the presented period, except for CWT ($n = 8$). The bar plot insets represent the growth-temperature correlation of each parameter for different pollution periods (as the color shaded area referred). Black crosses mark non-significant correlations with a significant level of 0.01. Different color shaded areas represent different pollution periods, they are Pre-pollution (1930–1959), Peak pollution (1960–1989) and Post-pollution (1990–2008) from left to right.

While latewood TCA showed no clear trends at either site, WB had below-average values in the 1970s and 1980s (LW TCA = 507 and 493, respectively) compared to the long-term average (LW $TCA_{1900–2008}$ = 559). Notably, WB showed the lowest full ring (EW+LW) median TCA in the 1980s (922) and highest in the 2000s (1121) when compared to the long-term average of 1022. In contrast, the earlywood, latewood and full ring TCA remained close to average throughout the Peak- and Post-pollution periods at SP2 (Fig. 7 g, h). The ratio of earlywood and latewood lumen area (LA) to TCA displayed little variability over time at both sites, except for SP2, which showed distinctly higher latewood values in the late 1970s. The ratio of latewood to earlywood TCA (LWTCA / EWTCA) averaged 50 % at WB, reaching the lowest levels in the 1970s (43.7 %) and highest levels in the 1990s (54.6 %). At SP2, this ratio was lower on average (37.1 %), with minimum levels also in the 1970s (32.9 %) and maximum levels in the 1920s (39.6 %).

4. Discussion

4.1. Growth trend divergence and pollution impact synchronization

Our results revealed significant growth trend divergence and climate signal disruption at a few specific sites during periods of peak pollution, which primarily affected RW chronologies. The prominent growth declines in RW observed around the 1980s were closely temporally synchronized and spatially aligned with pollution intensity, with the most pronounced effects occurring during the Peak pollution period at the NB and WB sites closest to the main pollution sources in Central Europe at that time (i.e., the Black Triangle area which covers northern and western Bohemia). Among the tree-ring parameters considered, RW is the most susceptible to pollution (Figs. 4–6, S10). The negative impacts of pollution on tree growth and particularly RW chronologies, especially in severely pollution-affected locations, including pollution-induced growth declines, climate signal disruption and tree mortality, are well-documented phenomena (e.g., Kandler and Innes, 1995; Kharuk et al.,

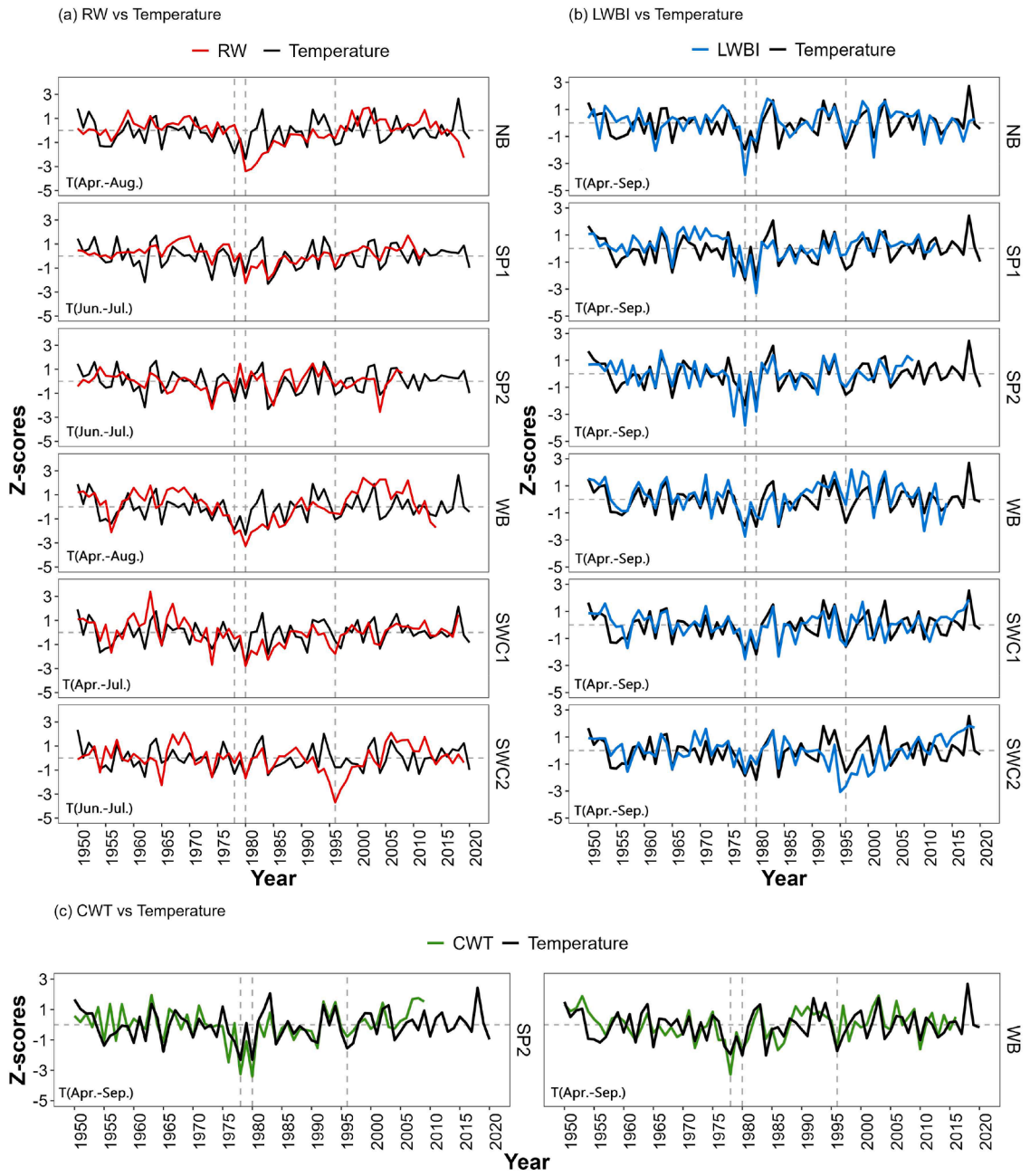

Fig. 6. Long-term trends comparison among tree-ring width (RW), latewood Blue Intensity (LWBI), and maximum cell wall thickness (CWT) chronologies and seasonal CRU temperature after 1950. All datasets are detrended using 80-year 'spline'. The optimal seasons were selected based on the highest seasonal correlations in Fig. 4 and Fig.S3 and are indicated in the panels for each site and parameter, with 'T' and the abbreviated month name representing mean temperature and the months of the year, e.g., T(Apr.-Aug.) corresponds to April-August mean temperature. To aid visual interpretation, the vertical dashed lines mark several distinct years (i.e., 1978, 1980, 1996) with prominent negative anomalies across all parameters and sites.

2023; Mathias and Thomas, 2018; Rydval and Wilson, 2012; Sidor et al., 2021; S. Vacek et al., 2015; Z. Vacek et al., 2020; Wilson & Elling, 2004).

A variety of plant physiological processes and increased soil acidification can either separately or jointly lead to the growth reductions observed in RW chronologies. High levels of pollutants can lead to a reduction in growth and productivity by causing injury to foliage and disrupting physiological processes, such as enzyme activity or production, stomatal closure and carbon allocation (Chappelka and Freer-Smith, 1995; Grill et al., 2005; Savard, 2010). Leaves directly exposed to pollutants (e.g., SO_2, NOx) experience faster water loss and increased transpiration due to accelerated cuticular degradation or disruption of the leaf epidermis. Although these conditions can also lead to higher water-use efficiency (Thomas et al., 2013; Treml et al., 2022), they ultimately reduce stomatal conductance and cause stomatal closure to prevent further water loss (Wright et al., 1987). This represents a mechanism by which high concentrations of SO_2 can severely limit growth rates (Kwak et al., 2016). Furthermore, increased soil acidification from acid deposition leads to the leaching of base cations from the soil-rooting zone, depleting the soil's ion-exchange capacity and inhibiting litter decomposition (Kolář et al., 2015), which hinders nutrient acquisition and assimilation necessary for tree growth (Oulehle et al., 2024).

It is also essential to consider that additional factors, such as unfavorable growing and dormant season conditions in the late 1970s and early 1980s, may have interacted with high background pollution levels to reduce growth. For example, several years with colder summers (e.g.,

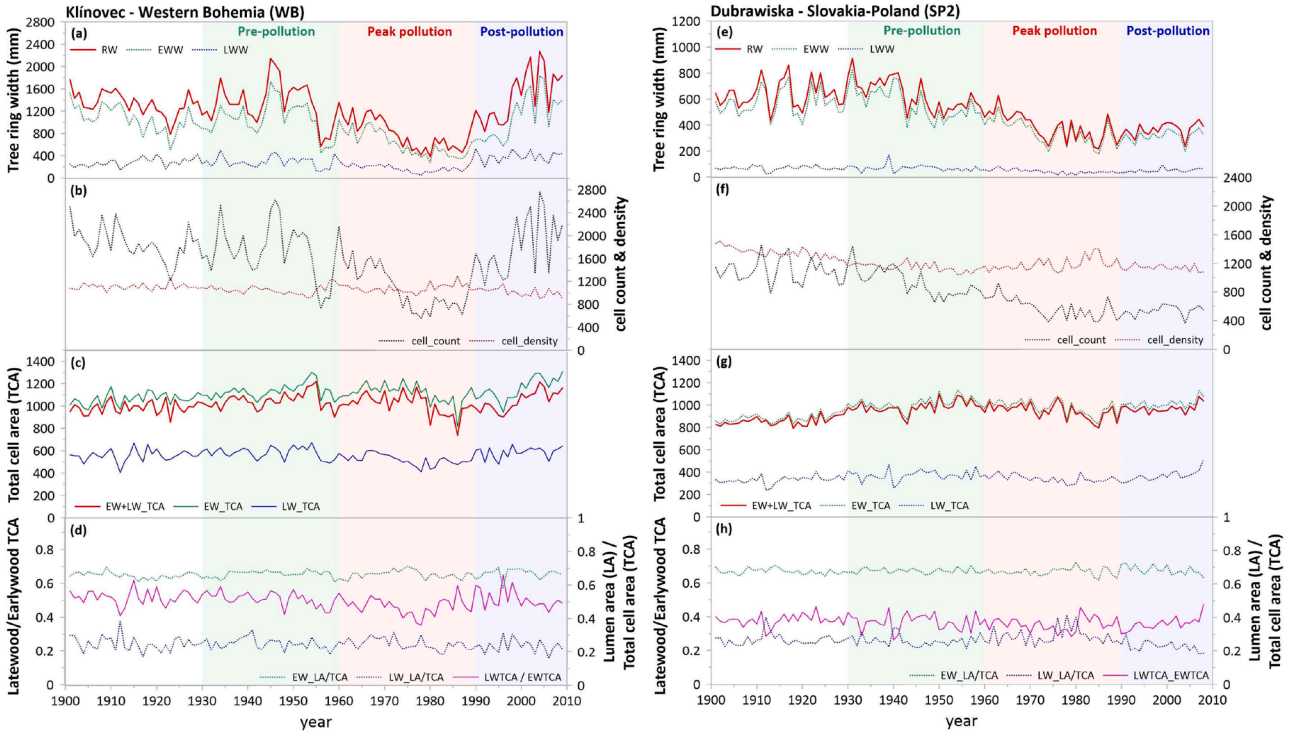

Fig. 7. Quantitative wood anatomical (QWA) parameters for West Bohemia (WB) and the Slovakia-Poland border (SP2), including **(a, e)** non-detrended median tree-ring width (RW), earlywood width (EWW) and latewood width (LWW), **(b, f)** average cell count and cell density (cell count per unit area), **(c, g)** median of total cell area for the earlywood (EW_TCA) and latewood (LW_TCA), and **(d, h)** ratios of median lumen area to total cell area for the earlywood (EW_LA/TCA) and latewood (LW_LA/TCA) along with the ratio of median latewood to earlywood total cell area (LWTCA / EWTCA). Note the scaling difference between panels **a, e** and **b, f**.

1980, Kroupová, 2002) or harsh winter conditions (e.g., the extremely cold winter of 1978–1979, Rein and Štekl, 1981; Majewski et al., 2011) created environments more conducive to air pollutant accumulation (Lomský et al., 2013), increasing stress and limiting recovery. Freezing temperatures, combined with high SO_2 concentrations, may have further exacerbated forest decline (Sheppard and Pfanz, 2001).

In contrast to RW, no clear deviations from instrumental temperatures were observed in the LWBI and CWT chronologies in the 1970s and 1980s and the timing and characteristics of the only LWBI decline, which occurred in the mid-1990s at SWC2, are intriguing (Fig. 2b; Fig. 7; Fig. S2b). Considering its occurrence after the Peak pollution period and being more prominent in LWBI compared to the moderate decline in RW, it is unlikely to be pollution-related. The winter of 1995 / 1996 was saw extreme conditions, including a sudden temperature drop in November 1995, followed by heavy frosts and prolonged inversion conditions (Samusevich et al., 2017; Čejková et al., 2009). While a climatic trigger outside the growing season is a plausible explanation, it seems unlikely as no similar deviations were observed in nearby SWC1 chronologies. This suggests a site-specific cause. Another possibility is sample twisting during coring, which could locally increase surface reflectivity. However, since a similar but less pronounced decline was also observed in the SWC2 RW chronology, the precise cause remains elusive. Further investigation would be necessary to determine if a site-specific event played a role.

The discrepancy between pollution loading and site impact may indicate that modelled pollution levels may not necessarily accurately represent the degree of impact on forest stands as various other factors can also play an important role (e.g., considering the seemingly similar pollution loading yet contrasting temperature signal patterns among SP1 / SP2 and NB / WB (Table 1; Figs. 5, 6). For example, lower correlations between ring width and temperature for sites located on slopes with more effective acid fog deposition were previously reported, and greater distance from the pollution source was associated with an increase in climatic sensitivity (Opała-Owczarek et al., 2019; Rydval and Wilson, 2012). Additionally, despite generally high background pollution levels, RW chronologies have been reported to be considerably less affected by pollution due to the blocking of wind-transported pollutants by the Tatra Mts. (Fig. 1; Chropeňová et al., 2016; Sekuła et al., 2021).

4.2. *Stability of temperature signals in tree-ring parameters from pollution-affected areas*

The growing season temperature signals represented by the three evaluated tree-ring parameters (RW, LWBI, CWT) concerning their seasonal length and climate signal strength varied considerably among sites and parameters. These signals (April-September for LWBI and CWT, and June-July or April-July / August for RW) generally agreed with previous studies of high-elevation conifer species throughout Central and Eastern Europe (Björklund et al., 2019; Büntgen and Di Cosmo, 2016; Horodnic and Roibu, 2020; Jiang et al., 2022; Putalová et al., 2019; Schurman et al., 2019). Most notably, the generally stronger, spatially more consistent and temporally broader seasonal temperature signals captured by LWBI and CWT indicated the higher climatic (i.e., temperature) sensitivity of these two parameters compared to RW.

One important finding is the observed temporal instability (i.e., signal weakening) in RW temperature signals at several sites, particularly within the Black Triangle, where the response weakened substantially or even disappeared during both the Peak pollution and Post-pollution periods, suggesting a higher susceptibility of RW chronologies in those areas to pollution stress. The retention of a comparatively stronger high-frequency temperature signal (Fig. S7) around the 1980s at those sites indicates that pollution-induced growth suppression played a major role in overall temperature signal disruption during the Peak pollution period. The subsequent complete decoupling between RW and temperature in the Post-pollution period remains unclear but may result from some combination of warming conditions and ecological disruption linked to pollution legacy effects.

In contrast to these declining signals at most Czech sites, RW

temperature signals at the Slovakia sites (and also SWC1) remained stronger and more stable throughout the study period. Interestingly, these sites are not only located farther from the main pollution sources in the Black Triangle but are also situated at higher elevations (>1300 m a.s.l.), which may contribute to their higher resilience. Additionally, sites in the Black Triangle were prone to winter inversions and acidic fog or rime exposure, which exacerbated pollution-related tree damage (Godek et al., 2015; Hruška et al., 2023). These factors highlight the difficulty in disentangling the direct effects of pollution, site-specific differences, post-pollution legacy impacts, climate change-related temperature signal weakening, and elevation (e.g., Kašpar et al., 2024; Kolář et al., 2015).

In contrast to RW, the temperature signals in LWBI and maximum CWT chronologies were not only much stronger but largely also considerably more temporally stable, showing no clear signs of disruption due to pollution (both in terms of chronology trends and temperature signal strength). Although a reduction in the LWBI temperature signal was observed at the two South-western Czechia sites in the most recent period (Fig. 5e, f), this weakening occurred predominantly during the post-pollution period, was not mirrored by the RW signal strength, and affected sites that were presumably exposed to the lowest pollution levels in the network (Table 1). Overall, particularly considering their strong performance at the most impacted sites (especially NB and WB), our findings indicate that both LWBI and CWT are more reliable and preferable climate proxies than RW for dendroclimatological research and historical climate reconstruction in pollution-affected areas.

4.3. Linkages between wood anatomical properties and tree-ring parameter responses to pollution

The changing patterns of QWA parameters revealed that cell count was the predominant control on RW chronology trends, with little to no indication of any anomalous patterns in anatomical properties of cells and their proportions such as cell density and cell area (Fig. 7). When trees are subjected to severe pollution stress, which replaced the climate as the dominant limiting factor of growth, significant damage to the foliage can disrupt wood formation by interfering with cambial activity and tracheid differentiation, affecting, among other factors, the number of cambial cells (Myśkow et al. 2019; Samusevich et al., 2017). Moreover, defoliation makes crowns smaller (similarly to suppressed trees), and such trees have lower numbers of cells in the cambial zone (Rathgeber et al., 2011; Liu et al., 2018), resulting in lower intensity of cambial division. Under the background of severe pollution stress, a reduction in the number of cells produced will inherently reduce ring width and manifested as a reduced response of tree growth to climatic factors. While stress-induced defoliation can lead to narrower annual rings, it has also been associated with the prioritization of resource allocation to latewood formation over earlywood (Sudachkova et al., 2015). Given that latewood development occurs later in the growing season, plays a structurally important role, and is more directly influenced by temperature conditions, the later phases of cell maturation which govern LWBI and maximum CWT may therefore remain relatively unaffected, retaining a more consistent climatic signal (Carrer et al., 2017; Rossi et al., 2008). This would help explain the observed retention of stronger and temporally more stable temperature signals in those parameters compared to RW. When severe pollution happened, it inevitably became the limiting factor for tree growth, led to reduced number of cells and overrode the climate signals which was especially reflected by RW.

These findings help explain why RW was so clearly affected during and after periods of pollution impact (marked by suppressed growth and growth release trends, respectively) at severely impacted sites WB and NB. In contrast, parameters representing density (LWBI), and anatomical properties (CWT and others) remained largely unaffected. Although some minor changes in anatomical properties (e.g., earlywood TCA and the LWTCA to EWTCA ratio) were identified during and after the Peak pollution period (Fig. 7c. g), particularly at the more impacted WB site, overall anatomical differences over time were limited. Most notably, the latewood parameters showed no clear alterations during these periods. This aligns with Myśkow et al. (2019) who found that highly polluted conditions caused modifications of earlywood but not latewood tracheid. Interestingly, both latewood density (LWBI) and wood anatomy (CWT) were also unaffected during the post-pollution period, as the growth release at the WB site was primarily driven by higher cell counts, resulting in unusually large ring widths but no disruption of latewood density and cell properties. These observations align with (and may help explain) the findings of Jiang et al. (2022), which showed that growth releases in response to disturbances considerably affected RW chronologies but did not influence the climatic signals or trends in LWBI datasets.

4.4. Parameter selection of climate reconstructions for pollution sites

From a dendroclimatic perspective, efforts to reduce, mitigate or circumvent pollution-related impacts on tree-ring chronologies are essential. The Curve Intervention Detection method used in this study offers a practical approach to identifying pollution-induced trend anomalies and reducing their influence on RW chronologies and associated temperature signals. While this approach cannot improve interannual signals, it can reduce trend distortion caused by growth suppression and any subsequent releases (Jiang et al., 2022; Rydval et al., 2015). In situations where obtaining multiple parameters is not feasible and RW datasets remain the only accessible option, the adoption of statistical approaches, such as the CID method, and their application to site chronologies with severe pollution impacts can help reduce protracted growth suppression trends in such datasets.

While some limited improvement of RW chronologies may be possible with such approaches, this study clearly demonstrates that the utilization of tree-ring parameters (such as LWBI and CWT) based on more sophisticated techniques (i.e. reflected light imaging or QWA) represents a better strategy for tree-ring research in areas affected by pollution, as their stronger, more temporally stable climatic signals, in addition to their insensitivity to pollution impacts, offer considerable benefits over RW. Although not directly examined in this study, parameters derived from X-ray densitometry (e.g., maximum latewood density – MXD) are likely to be unaffected by pollution similarly to LWBI. In the context of climate reconstruction development, care should be taken in selecting parameters and calibration periods, especially considering the potential instability of the climate signal in tree-ring width due to varying pollution levels over time. Appropriate measures should be taken to minimize such non-climatic influences and ensure the reliability of climate signals.

With society's industrial development, environmental pollution has become a matter of global concern, significantly impacting the health and development of forest ecosystems (Taylor et al., 1994). These issues are not confined to Europe (Kandler et al., 1995; Katzensteiner et al., 1992) but extend to forests in other parts of the world, such as North America (Johnson and Taylor, 1989; McLaughlin, 1998) and Asia (Izuta, 2017; Takahashi et al., 2020), with some locations (e.g., China and India) still experiencing high pollution levels due to ongoing heavy industrial activity. This research highlights the importance of considering the potential impacts of pollution in dendroclimatological context, especially in areas with a history of significant pollution exposure.

5. Conclusion

Our study investigated the impacts of the widespread high levels of pollution in Central Europe during the 1960s-1980s on Norway spruce growth trends and climatic sensitivity. Specifically, this study was conducted in the Czech Republic and the neighboring regions by utilizing a network of high-elevation Norway spruce sites and datasets of several tree-ring parameters. The examined tree-ring parameters

included tree-ring width (RW), latewood Blue Intensity (LWBI) derived from the Blue Intensity (BI) technique, as well as maximum tracheid cell wall thickness (CWT) using quantitative wood anatomy (QWA). Based on pollution history, we performed an assessment of the spatial and temporal extent of these impacts and how they influenced various tree-ring features. The impact of pollution on tree growth differed considerably among tree-ring parameters, which indicated their variable resilience to this influence. RW was generally more susceptible to pollution impact, which manifested as either trend divergence (i.e. suppression) and / or climate signal weakening, and these effects were most prominent at sites within the Black Triangle (i.e., NB and WB) area. We demonstrated that the Curve Intervention Detection (CID) method can help mitigate trend distortion to some extent, particularly for sites where the effect is most severe. However, the benefits of this approach may be limited.

Unlike RW, the reflected light imaging parameter LWBI and the wood anatomical parameter maximum CWT were less impacted by pollution, retaining stronger, seasonally broader, and temporally more stable temperature signals. This demonstrates that LWBI and maximum CWT not only represent stronger temperature proxies in general but also offer distinct advantages over RW in pollution-affected regions. The reason properly lies in that pollution (as the limiting factor for tree growth when severe pollution happened) primarily reduced the cell numbers (which was more related to RW) rather than lumen size or cell wall thickness and thus weakened RW's response to climate. However, LWBI and latewood CWT were related to latewood formation during reduced physiological activity growth period, and their climatic response was less likely to be influenced by pollution, making them more robust climate proxies in polluted regions. Beyond these parameters, future investigations involving climatic signals from tree-ring stable isotope chronologies ($\delta^{18}O$, $\delta^{13}C$), as well as patterns of other isotopes (e.g., $\delta^{15}N$ and $\delta^{34}S$) or trace elements such as sulfur and iron in tree rings from pollution-affected areas could provide further valuable insights into the impacts of pollution on trees. Furthermore, the potential impacts of pollution on tree growth in more moisture-limited lower-elevation and lower-latitude locations should also be examined in relation to the broad spectrum of available tree-ring parameters.

An important takeaway of this study is the need to consider pollution impacts on tree-ring datasets when conducting dendroclimatological research, particularly when using RW chronologies as the primary focus for climate signal assessments or dendroclimatic reconstructions in pollution-affected areas. Instead, whenever possible, we strongly recommend exploring and utilizing climatic signals from other tree-ring parameters, such as LWBI and maximum CWT, to capture stronger and more stable climatic signals.

CRediT authorship contribution statement

Yumei Jiang: Writing – original draft, Visualization, Validation, Software, Project administration, Methodology, Investigation, Funding acquisition, Formal analysis, Data curation, Conceptualization. **Krešimir Begović:** Writing – review & editing, Investigation, Data curation, Conceptualization. **Martin Lexa:** Writing – review & editing, Resources, Investigation, Data curation. **Juliana Nogueira:** Writing – review & editing, Investigation, Data curation. **Georg von Arx:** Writing – review & editing, Software, Resources, Methodology, Data curation, Conceptualization. **Jan Tumajer:** Writing – review & editing, Methodology, Data curation, Conceptualization. **Ryszard Kaczka:** Writing – review & editing, Resources. **Filip Oulehle:** Writing – review & editing, Data curation. **Nataliya Korolyova:** Writing – review & editing, Resources, Data curation. **Jesper Björklund:** Writing – review & editing, Methodology. **Kristina Seftigen:** Writing – review & editing, Methodology. **Vaclav Treml:** Writing – review & editing, Methodology. **Rob Wilson:** Writing – review & editing, Methodology. **Miloš Rydval:** Writing – original draft, Visualization, Supervision, Resources, Project administration, Methodology, Investigation, Funding acquisition, Data curation, Conceptualization.

Declaration of competing interest

The authors declare that they have no known competing financial interests or personal relationships that could have appeared to influence the work reported in this paper.

Acknowledgements

This research was undertaken as part of the REPLICATE project (20-22351Y) funded by the Czech Science Foundation (GAČR), as well as by the Czech University of Life Sciences Prague institutional project (IGA Grant funding 2022/2023, project No A_21_22). JT was supported by Charles University [PRIMUS/24/SCI/004] and Programme JAC [CZ.02.01.01/00/22_008/0004605]. JB received funding from the SNF Sinergia project CALDERA (no.183571). JB and GvA received funding from the SNF project XELLCLIM (no. 200021_182398). We are grateful to the technicians from the dendro-ecological laboratory and the MultiDendro laboratory at the Department of Forest Ecology, Czech University of Life Sciences Prague for helping with sample collection, tree-ring width data measurement, cross-dating, sample scanning and BI data generation. We also acknowledge colleagues L. Schneider and D. Nievergelt of the Dendrosciencies Research Group in the Swiss Federal Institute for Forest, Snow and Landscape Research WSL (Birmensdorf, Switzerland) for their guidance and assistance in wood anatomy-related experiments.

Supplementary materials

Supplementary material associated with this article can be found, in the online version, at doi:10.1016/j.agrformet.2025.110725.

Data availability

Data will be made available on request.

References

Abraham, J., Berger, F., Ciechanowicz-Kusztal, R., Jodłowska-Opyd, G., Kallweit, D., Keder, J., Kulaszka, W., Novák, J., 2002. Common report on air quality in the black triangle region 2002. https://www.wroclaw.wios.gov.pl/pliki/miedzynarodowe/raport2002.pdf.

Bäck, J., Huttunen, S., Turunen, M., Lamppu, J., 1995. Effects of acid rain on growth and nutrient concentrations in Scots pine and Norway spruce seedlings grown in a nutrient-rich soil. Environ. Pollut. 89 (2), 177–187.

Büntgen, U., Di Cosmo, N., 2016. Climatic and environmental aspects of the Mongol withdrawal from Hungary in 1242 ce. Sci. Rep. 6 (February), 1–9. https://doi.org/10.1038/srep25606.

Bangdiwala, S.I., 2018. Regression: simple linear. Int. J. Inj. Contr. Saf. Promot. 25 (1), 113–115.

Björklund, J., Rydval, M., Schurman, J.S., Seftigen, K., Trotsiuk, V., Janda, P., Mikoláš, M., Dušátko, M., Čada, V., Bače, R., Svoboda, M., 2019. Disentangling the multi-faceted growth patterns of primary Picea abies forests in the Carpathian arc. Agric. For. Meteorol. 271 (October 2018), 214–224. https://doi.org/10.1016/j.agrformet.2019.03.002.

Björklund, J., Seftigen, K., Fonti, P., Nievergelt, D., von Arx, G., 2020. Dendroclimatic potential of dendroanatomy in temperature-sensitive Pinus sylvestris. Dendrochronologia 60 (February). https://doi.org/10.1016/j.dendro.2020.125673.

Björklund, J., Seftigen, K., Stoffel, M., Fonti, M.V., Kottlow, S., Frank, D.C., von Arx, G., 2023. Fennoscandian tree-ring anatomy shows a warmer modern than medieval climate. Nature 620 (7972), 97–103.

Björklund, J., Seftigen, K., Kaczka, R.J., Rydval, M., Wilson, R., 2024. A definition and standardised terminology for blue intensity from conifers. Dendrochronologia 85, 126200.

Borůvka, L., Podrázský, V., Mládková, L., Kuneš, I., Drábek, O., 2005. Some approaches to the research of forest soils affected by acidification in the Czech Republic. Soil Sci. Plant Nutrit. 51 (5), 745–749.

Bunn, A., Korpela, M., Biondi, F., Campelo, F., Mérian, P., Qeadan, F., Klesse, S., 2015. Package 'dplR'. Dendrochronology Program Library in R, Version 1 (3).

Čejková, A., Čejková, A., Kolář, T., 2009. Extreme radial growth reaction of norway spruce along an altitudinal gradient in the Šumava Mountains. Geochronometria 33 (1), 41–47. https://doi.org/10.2478/v10003-009-0012-6.

Campbell, R., McCarroll, D., Robertson, I., Loader, N.J., Grudd, H., Gunnarson, B., 2011. Blue intensity in Pinus sylvestris tree rings: a manual for a new palaeoclimate proxy. Tree Ring. Res. 67 (2), 127–134.
Carrer, M., Castagneri, D., Prendin, A.L., Petit, G., von Arx, G., 2017. Retrospective analysis of wood anatomical traits reveals a recent extension in tree cambial activity in two high-elevation conifers. Front. Plant Sci. 8, 737. https://doi.org/10.3389/fpls.2017.00737.
Chappelka, A.H., Freer-Smith, P.H., 1995. Predisposition of trees by air pollutants to low temperatures and moisture stress. Environ. Pollut. 87 (1), 105–117. https://doi.org/10.1016/S0269-7491(99)80013-X.
Chropeňová, M., Gregušková, E.K., Karásková, P., Přibylová, P., Kukučka, P., Baráková, D., Čupr, P., 2016. Pine needles and pollen grains of pinus mugo turra–a biomonitoring tool in high mountain habitats identifying environmental contamination. Ecol. Indic. 66, 132–142.
Cook, E.R., Peters, K., 1997. Calculating unbiased tree-ring indices for the study of climatic and environmental change. Holocene 7 (3), 361–370.
Dignon, J., Hameed, S., 1989. Historic emissions ofsulfur and nitrogen oxides from1860 to 1980. J. Air Pollut. Control Assoc. 39, 180–186.
Druckenbrod, D.L., Pederson, N., Rentch, J., Cook, E.R., 2013. A comparison of times series approaches for dendroecological reconstructions of past canopy disturbance events. Forest Ecol. Manag. 302, 23–33. https://doi.org/10.1016/j.foreco.2013.03.040.
Druckenbrod, D.L., 2005. Dendroecological reconstructions of forest disturbance history using time-series analysis with intervention detection. Can. J. For. Res. 35 (4), 868–876. https://doi.org/10.1139/x05-020.
Edwards, J., Anchukaitis, K.J., Gunnarson, B.E., Pearson, C., Seftigen, K., von Arx, G., Linderholm, H.W., 2022. The origin of tree-ring reconstructed summer cooling in northern Europe during the 18th century eruption of Laki. Paleoceanogr. Paleoclimatol. 37 (2), e2021PA004386.
Engardt, M., Simpson, D., Schwikowski, M., Granat, L., 2017. Deposition of sulphur and nitrogen in Europe 1900–2050. Model calculations and comparison to historical observations. Tellus, Series B 69 (1), 1–20. https://doi.org/10.1080/16000889.2017.1328945.
Fuentes, M., Björklund, J., Seftigen, K., Salo, R., Gunnarson, B.E., Linderholm, H.W., & Aravena, J.C. (2016). A comparison between tree-ring width and blue intensity high and low frequency signals from Pinus sylvestris l. from the Central and Northern Scandinavian Mountains. STR16/04, 38.
Gärtner, H., Lucchinetti, S., Schweingruber, F.H., 2015. A new sledge microtome to combine wood anatomy and tree-ring ecology. IAWa J. 36 (4), 452–459.
Godek, M., Sobik, M., Błaś, M., Polkowska, Ż., Owczarek, P., Bokwa, A., 2015. Tree rings as an indicator of atmospheric pollutant deposition to subalpine spruce forests in the Sudetes (Southern Poland). Atmos. Res. 151, 259–268.
Grill, D., Pfanz, H., Lomsky, B., Bytnerowicz, A., Grulke, N.E., Tausz, M., 2005. Physiological responses of trees to air pollutants at high elevation sites. Plant ResponsesAir Pollut. Glob. Change 37–44. https://doi.org/10.1007/4-431-31014-2_5.
Grubler, A., 2002. Trends in global emissions: carbon, sulfur, and nitrogen. Encyclopedia Glob. Environ. Change 3 (May), 35–53.
Hůnová, I., Šantroch, J., Ostatnická, J., 2004. Ambient air quality and deposition trends at rural stations in the Czech Republic during 1993–2001. Atmos. Environ. 38 (6), 887–898.
Harris, I., Osborn, T.J., Jones, P., Lister, D., 2020. Version 4 of the cru ts monthly high-resolution gridded multivariate climate dataset. Sci. Data 7 (1), 109.
Heeter, K.J., Harley, G.L., Van De Gevel, S.L., White, P.B., 2019. Blue intensity as a temperature proxy in the eastern United States: a pilot study from a southern disjunct population of Picea rubens (Sarg.). Dendrochronologia 55, 105–109.
Heeter, K.J., King, D.J., Harley, G.L., Kaczka, R.J., 2022. Video tutorial: measuring blue intensity with the coorecorder software application. Dendrochronologia 76, 125999.
Horodnic, S.A., Roibu, C.C., 2020. Collective growth patterns reveal the high growing potential of older silver fir trees in a primeval forest in Romania's Southern Carpathians. Not Bot Horti Agrobot Cluj Napoca 48 (2), 1085–1099. https://doi.org/10.15835/nbha48211949.
Hruška, J., Oulehle, F., Chuman, T., Kolář, T., Rybníček, M., Trnka, M., McDowell, W.H., 2023. Forest growth responds more to air pollution than soil acidification. PLoS One 18 (3 March), 1–21. https://doi.org/10.1371/journal.pone.0256976.
Izuta, T. (Ed.), 2017. Air Pollution Impacts On Plants in East Asia. Springer.
Jiang, Y., Begović, K., Nogueira, J., Schurman, J.S., Svoboda, M., Rydval, M., 2022. Impact of disturbance signatures on tree-ring width and blue intensity chronology structure and climatic signals in Carpathian Norway spruce. Agric. For. Meteorol. 327 (March). https://doi.org/10.1016/j.agrformet.2022.109236.
Johnson, D.W., Taylor, G.E., 1989. Role of air pollution in forest decline in eastern North America. Water Air Soil Pollut. 48, 21–43.
Kašpar, J., Tumajer, J., Altman, J., Altmanova, N., Čada, V., Čihák, T., Treml, V., 2024. Major tree species of Central European forests differ in their proportion of positive, negative, and nonstationary growth trends. Glob. Chang. Biol. 30 (1), e17146.
Kandler, O., Innes, J.L., 1995. Air pollution and forest decline in Central Europe. Environ. Pollut. 90 (2), 171–180. https://doi.org/10.1016/0269-7491(95)00006-D.
Katzenmaier, M., Garnot, V.S.F., Björklund, J., Schneider, L., Wegner, J.D., von Arx, G., 2023. Towards Roxas AI: deep learning for faster and more accurate conifer cell analysis. Dendrochronologia 81, 126126.
Katzensteiner, K., Glatzel, G., Kazda, M., Sterba, H., 1992. Effects of air pollutants on mineral nutrition of Norway spruce and revitalization of declining stands in Austria. Water Air Soil Pollut. 61, 309–322.
Kharuk, V.I., Petrov, I.A., Im, S.T., Golyukov, A.S., Dvinskaya, M.L., Shushpanov, A.S., 2023. Pollution and climatic influence on trees in the Siberian Arctic wetlands. Water 15 (2), 215. https://doi.org/10.3390/w15020215.
Kirdyanov, A.V., Krusic, P.J., Shishov, V.V., Vaganov, E.A., Fertikov, A.I., Myglan, V.S., Büntgen, U., 2020. Ecological and conceptual consequences of arctic pollution. Ecol. Lett. 23 (12), 1827–1837.
Kolář, T., Čermák, P., Oulehle, F., Trnka, M., Štěpánek, P., Cudlín, P., Hruška, J., Büntgen, U., Rybníček, M., 2015. Pollution control enhanced spruce growth in the "Black triangle" near the Czech-polish border. Sci. Total Environ. 538, 703–711. https://doi.org/10.1016/j.scitotenv.2015.08.105.
Kopáček, J., Veselý, J., 2005. Sulfur and nitrogen emissions in the Czech Republic and Slovakia from 1850 till 2000. Atmos. Environ. 39 (12), 2179–2188. https://doi.org/10.1016/j.atmosenv.2005.01.002.
Krejcí, F., Vacek, S., Bílek, L., Mikeska, M., Hejcmanová, P., Vacek, Z., 2013. The effects of climatic conditions and forest site types on disintegration rates in Picea abies occurring at the Modrava Peat Bogs in the Šumava national park. Dendrobiology (70).
Kroupová, M., 2002. Dendroecological study of spruce growth in regions under long-term air pollution load. Journal of Forest Science 48 (12), 536–548.
Kwak, J.H., Lim, S.S., Lee, K.S., Viet, H.D., Matsushima, M., Lee, K.H., Jung, K., Kim, H. Y., Lee, S.M., Chang, S.X., Choi, W.J., 2016. Temperature and air pollution affected tree ring δ13C and water-use efficiency of pine and oak trees under rising CO2 in a humid temperate forest. Chem. Geol. 420, 127–138. https://doi.org/10.1016/j.chemgeo.2015.11.015.
Liu, S., Li, X., Rossi, S., Wang, L., Li, W., Liang, E., Leavitt, S.W., 2018. Differences in xylogenesis between dominant and suppressed trees. Am. J. Bot. 105 (5), 950–956.
Lomský, B., Šrámek, V., Novotný, R., 2013. The health and nutritional status of Norway spruce stands in the Krušné hory MTS. 15 years subsequent to the extreme winter of 1995/96. J. Forest Sci. 59 (9), 359–369.
Lopez-Saez, J., Corona, C., Von Arx, G., Fonti, P., Slamova, L., Stoffel, M., 2023. Tree-ring anatomy of pinus cembra trees opens new avenues for climate reconstructions in the European alps. Sci. Total Environ. 855, 158605.
Majewski, G., Gołaszewski, D., Przewoźniczuk, W., Rozbicki, T., 2011. Warunki termiczne i śnieżne zim w Warszawie w latach 1978/79–2009/10. Prac. Studi. Geograf. 47, 147–155.
Mathias, J.M., Thomas, R.B., 2018. Disentangling the effects of acidic air pollution, atmospheric CO2, and climate change on recent growth of red spruce trees in the Central Appalachian mountains. Glob. Chang. Biol. 24 (9), 3938–3953. https://doi.org/10.1111/gcb.14273.
Maxwell, R.S., Larsson, L.A., 2021. Measuring tree-ring widths using the Coorecorder software application. Dendrochronologia 67, 125841.
McLaughlin, D., 1998. A decade of forest tree monitoring in Canada: evidence of air pollution effects. Environmental Reviews 6 (3–4), 151–171.
Modrzyński, J., 2003. Defoliation of older Norway spruce (Picea abies/L./Karst.) stands in the polish Sudety and Carpathian mountains. Forest Ecol. Manag. 181 (3), 289–299.
Moldan, B., Schnoor, J.L., 1992. Czechoslovakia: examining a critically ill environment. Environ. Sci. Technol. 26 (1), 14–21.
Myśkow, E., Błaś, M., Sobik, M., Godek, M., Owczarek, P., 2019. The effect of pollutant fog deposition on the wood anatomy of subalpine Norway spruce. Eur. J. For. Res. 138, 187–201.
Ols, C., Klesse, S., Girardin, M.P., Evans, M.E., DeRose, R.J., Trouet, V., 2023. Detrending climate data prior to climate–growth analyses in dendroecology: a common best practice? Dendrochronologia 79, 126094.
Opała-Owczarek, M., Błaś, M., Owczarek, P., Sobik, M., Godek, M., 2019. A dendroclimatological study of east- and west-facing slopes in mountainous areas subjected to strong air pollution (the Sudetes, Central Europe). Phys. Geogr. 40 (2), 186–208. https://doi.org/10.1080/02723646.2018.1547872.
Oulehle, F., Kopáček, J., Chuman, T., Černohous, V., Hůnová, I., Hruška, J., Krám, P., Lachmanová, Z., Navrátil, T., Štěpánek, P., Tesař, M., Evans, C.D., 2016. Predicting sulphur and nitrogen deposition using a simple statistical method. Atmos. Environ. 140, 456–468. https://doi.org/10.1016/j.atmosenv.2016.06.028.
Oulehle, F., Kolář, T., Rybníček, M., Hruška, J., Büntgen, U., Trnka, M., 2024. Complex imprint of air pollution in the basal area increments of three european tree species. Sci. Total Environ. 951, 175858.
Ponocná, T., Chuman, T., Rydval, M., Urban, G., Migała, K., Treml, V., 2018. Deviations of treeline Norway spruce radial growth from summer temperatures in East-Central Europe. Agric. For. Meteorol. 253, 62–70.
Putalová, T., Vacek, Z., Vacek, S., Štefančík, I., Bulušek, D., Král, J., 2019. Tree-ring widths as an indicator of air pollution stress and climate conditions in different Norway spruce forest stands in the Krkonoše MTS. Central European Forestry Journal 65 (1), 21–33. https://doi.org/10.2478/forj-2019-0004.
Rein, F., Štekl, J., 1981. The extremeness of the cold front of Dec. 31, 1978 over the CSR. Travaux géophysiques 29, 379–404.
Rossi, S., Deslauriers, A., Anfodillo, T., Carrer, M., 2008. Age-dependent xylogenesis in timberline conifers. New Phytol. 177, 199–208. https://doi.org/10.1111/j.1469-8137.2007.02235.x.
Rydval, M., Wilson, R., 2012. The impact of industrial SO_2 pollution on north Bohemia conifers. Water Air Soil Pollut. 223, 5727–5744.
Rydval, M., Druckenbrod, D., Anchukaitis, K.J., Wilson, R., 2015. Detection and removal of disturbance trends in tree-ring series for dendroclimatology. Can. J. For. Res. 46 (3), 387–401. https://doi.org/10.1139/cjfr-2015-0366.
Rydval, M., Druckenbrod, D.L., Svoboda, M., Trotsiuk, V., Janda, P., Mikoláš, M., Čada, V., Bače, R., Teodosiu, M., Wilson, R., 2018. Influence of sampling and disturbance history on climatic sensitivity of temperature-limited conifers. Holocene 28 (10), 1574–1587. https://doi.org/10.1177/0959683618782605.
Šrámek, V., Slodičák, M., Lomský, B., Balcar, V., Kulhavý, J., Hadaš, P., Sloup, M., 2008. The ore mountains: will successive recovery of forests from lethal disease be successful. Mt. Res. Dev. 28 (3), 216–221.

Samusevich, A., Zeidler, A., & Vejpustková, M. (2017). Influence of air pollution and extreme frost on wood cell parameters at mountain spruce stands (Picea abies (L.) karst.) in the Ore mountains. Wood Research, 62(1), 79–90.

Savard, M.M., 2010. Tree-ring stable isotopes and historical perspectives on pollution - an overview. Environ. Pollut. 158 (6), 2007–2013. https://doi.org/10.1016/j.envpol.2009.11.031.

Schurman, J.S., Babst, F., Björklund, J., Rydval, M., Bače, R., Čada, V., Janda, P., Mikolas, M., Saulnier, M., Trotsiuk, V., Svoboda, M., 2019. The climatic drivers of primary Picea forest growth along the Carpathian arc are changing under rising temperatures. Glob. Chang. Biol. 25 (9), 3136–3150. https://doi.org/10.1111/gcb.14721.

Seftigen, K., Fonti, M.V., Luckman, B., Rydval, M., Stridbeck, P., Von Arx, G., Björklund, J., 2022. Prospects for dendroanatomy in paleoclimatology–a case study on picea engelmannii from the Canadian rockies. Climate of the Past Discussions 2022, 1–32.

Sekuła, P., Bokwa, A., Bartyzel, J., Bochenek, B., Chmura, Ł., Gałkowski, M., Zimnoch, M., 2021. Measurement report: effect of wind shear on PM 10 concentration vertical structure in the urban boundary layer in a complex terrain. Atmos. Chem. Phys. 21 (15), 12113–12139.

Sheppard, L., Pfanz, H., 2001. Impacts of Air Pollutants On Cold Hardiness. Springer Netherlands, pp. 335–366.

Sherman, R.E., Fahey, T.J., 1994. The effects of acid deposi- tion on the biogeochemical cycles ofmajor nutrients in min- iature red spruce ecosystems. Biogeochemistry 24, 85–114.

Sidor, C.G., Vlad, R., Popa, I., Semeniuc, A., Apostol, E., Badea, O., 2021a. Impact of industrial pollution on radial growth of conifers in a former mining area in the eastern carpathians (Northern romania). Forests 12 (5), 1–11. https://doi.org/10.3390/f12050640.

Slovik, S., Siegmund, A., Kindermann, G., Riebeling, R., Balázs, Á., 1995. Stomatal so 2 uptake and sulfate accumulation in needles of Norway spruce stands (Picea abies) in Central Europe. Plant Soil 168, 405–419.

Smil, V., et al., 1990. Nitrogen and phosphorus. In: Turner, B.L., et al. (Eds.), The Earth as Transformed by Human Action. Cambridge University Press, New York, pp. 423–436.

Sudachkova, N.E., Milyutina, I.L., Romanova, L.I., Astrakhantseva, N.V., 2015. Effect of defoliation on the growth and metabolism of Scots pine. Contemp. Probl. Ecol. 8, 21–27.

Takahashi, M., Feng, Z., Mikhailova, T.A., Kalugina, O.V., Shergina, O.V., Afanasieva, L. V., Heng, R.K.J., Majid, N.M.A., Sase, H., 2020. Air pollution monitoring and tree and forest decline in East Asia: a review. Sci. Total Environ. 742, 140288. https://doi.org/10.1016/j.scitotenv.2020.140288.

Taylor, G.E., Johnson, D.W., Andersen, C.P., 1994. Air pollution and forest ecosystems: a regional to global perspective. Ecol. Appl. 4 (4), 662–689.

Thomas, R.B., Spal, S.E., Smith, K.R., Nippert, J.B., 2013. Evidence of recovery of juniperus virginiana trees from sulfur pollution after the clean air act. Proc. Natl. Acad. Sci. USA 110 (38), 15319–15324. https://doi.org/10.1073/pnas.1308115110.

Treml, V., Mašek, J., Tumajer, J., Rydval, M., Čada, V., Ledvinka, O., Svoboda, M., 2022. Trends in climatically driven extreme growth reductions of picea abies and pinus sylvestris in central Europe. Glob. Chang. Biol. 28 (2), 557–570. https://doi.org/10.1111/gcb.15922.

Vacek, S., Hůnová, I., Vacek, Z., Hejcmanová, P., Podrázský, V., Král, J., Putalová, T., Moser, W.K., 2015. Effects of air pollution and climatic factors on Norway spruce forests in the Orlické hory MTS. (Czech Republic), 1979–2014. Eur. J. For. Res. 134 (6), 1127–1142. https://doi.org/10.1007/s10342-015-0915-x.

Vacek, S., Vacek, Z., Ulbrichová, I., Remeš, J., Podrázský, V., Vach, M., Putalová, T., 2019. The effects of fertilization on the health status, nutrition and growth of Norway spruce forests with yellowing symptoms. Scand. J. For. Res. 34 (4), 267–281.

Vacek, Z., Vacek, S., Prokůpková, A., Bulušek, D., Podrázský, V., Hůnová, I., Putalová, T., Král, J., 2020. Long-term effect of climate and air pollution on health status and growth of Picea abies (L.) Karst. Peaty forests in the black triangle region. Dendrobiology 83, 1–19. https://doi.org/10.12657/denbio.083.001.

von Arx, G., Carrer, M., 2014. Roxas -A new tool to build centuries-long tracheid-lumen chronologies in conifers. Dendrochronologia 32 (3), 290–293. https://doi.org/10.1016/j.dendro.2013.12.001.

Von Arx, G., Crivellaro, A., Prendin, A.L., Čufar, K., Carrer, M., 2016. Quantitative wood anatomy—Practical guidelines. Front. Plant Sci. 7 (JUNE2016), 1–13. https://doi.org/10.3389/fpls.2016.00781.

Wright, E.A., Lucas, P.W., Cottam, D.A., Mansfield, T.T., 1987. Physiological responses to SO2, NOx and O3: implications for drought resistance. direct effects of dry and wet deposition on forest ecosystems–in particular canopy interaction. CEC air pollut. Res. Rep 4, 187–200.

Zang, C., Biondi, F., 2015. Treeclim: an r package for the numerical calibration of proxy-climate relationships. Ecography 38 (4), 431–436. https://doi.org/10.1111/ecog.01335.